Keywords Argyrophilic grains · Hippocampal sclerosis · Progressive supranuclear palsy · Tau · TDP-43

Introduction

Transactivation-responsive DNA-binding protein of M_r 43 kDa (TDP-43) is a nuclear protein involved in transcriptional repression and alternative splicing. It was originally identified as a major component of ubiquitin-positive and tau-negative inclusions in the frontotemporal cortex and motor neurons in frontotemporal lobar degeneration (FTLD-U), with or without progranulin gene mutations, and in amyotrophic lateral sclerosis (ALS) [3, 12, 31]. Subsequent studies revealed that TDP-43 is also abnormally accumulated in familial FTLD-U with mutations in the valosin-containing protein gene [32], in familial FTLD with motor neuron disease linked to chromosome 9p [10], and in ALS with TDP-43 gene mutations [25, 38, 41, 44]. TDP-43 is considered to play an essential pathogenic role in these diseases, now-called TDP-43 proteinopathies.

Although TDP-43 accumulation was originally considered to be a specific disease marker for FTLD-U and ALS, subsequent studies demonstrated that abnormal TDP-43 accumulation in some cases of other neurodegenerative diseases, such as Alzheimer's disease (AD) [2], Parkinson's disease with and without dementia [30], dementia with Lewy bodies (DLB) + AD [4, 30], ALS/parkinson-dementia complex of Guam (ALS/PDC of Guam) [15, 16], argyrophilic grain disease (AGD) [14], and Huntington disease [37]. However, the pathophysiological significance of concurrent TDP-43 accumulation, and its impact on clinical phenotype in these diseases remain unclear.

Several previous studies have suggested that cases of progressive supranuclear palsy (PSP) lack abnormal TDP-43 accumulation [3, 18, 40]. In these early studies, phosphorylation-independent antibodies were employed in TDP-43 immunohistochemistry and immunoblot analysis. We have made polyclonal and monoclonal antibodies specific for phophorylated TDP-43, which identify phosphorylation sites in the C-terminus of the TDP-43 accumulated in FTLD-TDP brains [17, 20], and selectively immunolabel pathological inclusions and dystrophic neurites without physiological nuclear staining in FTLD-TDP, ALS, AD with TDP-43 pathology, and in DLB with TDP-43 [4, 17]. They also recognize hyperphosphorylated TDP-43 at 45 kDa and additional 18–26 kDa fragments in sarkosyl-insoluble fractions on immunoblotting.

The principal aim of this study was to revisit the presence or absence, and the frequency, of TDP-43 pathology in PSP cases using a phosphorylation-dependent anti-TDP-43 antibody. In contrast to previous reports, we demonstrated that a significant proportion of PSP cases had variable degrees of TDP-43 pathology in the limbic system. We subsequently examined the relationships between TDP-43 pathology, tau pathology, and hippocampal sclerosis, as well as biochemical nature of the abnormally accumulated TDP-43, in PSP.

Materials and methods

Subjects

We investigated 19 pathologically confirmed PSP cases, 12 pathologically confirmed corticobasal degeneration (CBD) cases and 4 pathologically normal control subjects (Table 1). These cases were obtained from UK Parkinson's Disease Society Tissue Bank (7 PSP and 4 control cases), Department of Pathology, Northwestern University Feinberg School of Medicine Cognitive Neurology and Alzheimer Disease Center (5 PSP and 7 CBD cases), and Department of Neuropsychiatry, Okayama University Graduate School of Medicine, Dentistry and Pharmaceutical Sciences (7 PSP and 5 CBD cases). All brains had been collected with Local Research Ethical Committee approval. All PSP cases showed characteristic tufted astrocytes, and all CBD cases astrocytic plaques, as revealed by Gallyas-Braak silver methods and tau immunohistochemistry.

Immunohistochemistry

Sections cut at 5-μm thickness to include the amygdala, entorhinal cortex, hippocampus, occipitotemporal cortex in all cases, as well as the substantia nigra in two cases for which tissue was available, were stained with antibodies against phosphorylated TDP-43 (pAb pS409/410, rabbit, polyclonal, 1:1,000 [17]), phosphorylated tau (AT8, mouse, monoclonal, 1:3,000, Innogenetics, Ghent, Belgium), phosphorylated α-synuclein (#1175, rabbit, polyclonal, 1:1,000, [33]), and Aβ (4G8, mouse, monoclonal, 1:2,000, Covance Research Products Inc., Dedham, MA, USA). Deparaffinized sections were incubated with 1% H_2O_2 in methanol for 20 min to eliminate endogenous peroxidase activity in the tissue. When using anti-α-synuclein and anti-TDP-43 antibodies, sections were pretreated to enhance immunoreactivity in a microwave oven for 5 min in 10 mM sodium citrate buffer, pH 6.0, at 100°C. After blocking with 10% normal serum, sections were incubated 1 h at room temperature with the primary antibody. After three 5-min washes in phosphate-buffered saline (PBS), sections were incubated in biotinylated secondary antibody for 30 min, and then in avidin-biotinylated horseradish peroxidase complex (ABC Elite kit, Vector, Burlingame, CA, USA) for

Table 1 Demographic data in PSP and CBD cases with and without TDP-43 pathologies

	PSP			CBD		
	All	TDP-43-positive PSP	TDP-43-negative PSP	All	TDP-43-positive CBD	TDP-43-negative CBD
N (%)	19	5 (26.3)	14 (73.7)	12	2 (16.7)	10 (83.3)
Male [*N* (%)]	16 (84.2)	4 (80.0)	12 (85.7)	7 (58.3)	1 (50.0)	6 (60.0)
Age at onset [mean (SD)]	68.3 (9.8)	75.0 (9.4)	65.7 (9.0)	55.2 (10.2)	49.0 (12.7)	56.6 (9.9)
Age at death [mean (SD)]	76.3 (10.7)	82.4 (11.7)	74.1 (9.8)	62.8 (11.2)	56.0 (15.6)	64.1 (10.7)
Duration [mean (SD)]	7.4 (4.4)	7.4 (4.6)	7.5 (4.6)	7.3 (2.9)	7.0 (2.8)	7.3 (3.1)
Dementia (%)	11 (57.9)	4 (80.0)	7 (50.0)	11 (91.7)	2 (100.0)	9 (90.0)
Brain weight [g, mean (SD)]	1,202 (142)	1,234 (180)	1,190 (132)	1,174 (146)	1,008 (152)	1,215 (120)
Argyrophilic grains [*N* (%)]	4 (21.1)	1 (20.0)	3 (21.4)	3 (25.0)	1 (50.0)	2 (20.0)
Hippocampal sclerosis [*N* (%)]	3 (15.8)	3 (60.0)	0 (0.0)	0 (0.0)	0 (0.0)	0 (0.0)

30 min. The peroxidase labeling was visualized with 0.2% 3,3′-diaminobenzidine (DAB) as chromogen. Sections were lightly counterstained with hematoxylin.

Semiquantitative assessment

TDP-43, tau, and Aβ pathologies in the amygdala, anterior and posterior portions of the entorhinal cortex, hippocampal dentate gyrus, CA1, 2, 3, and 4 regions, subiculum, fusiform gyrus, occipitotemporal gyrus were semiquantitatively evaluated using the following grading system blinded to any clinical or pathological information:

1. The total number of TDP-43-positive neuronal cytoplasmic inclusions (NCIs) in each anatomical region was assessed as follows: − no lesion, + one inclusion, ++ two or three inclusions, +++ four or five inclusions, ++++ 6–10 inclusions, +++++ 11 or over inclusions. In addition, the presence or absence of neuronal intranuclear inclusions (NIIs) and dystrophic neurites was also assessed. Then, we classified the topographic distribution of TDP-43 pathological changes using following system, which is similar to that reported by Amador-Ortiz et al. [2]: the amygdala type: inclusions were present only in the amygdala; the limbic type: inclusions extend to the amygdala, hippocampal dentate gyrus, CA1-4, entorhinal cortex, and fusiform gyrus, but not in the occipitotemporal gyrus; the temporal type: inclusions are present in the limbic system and also the in the occipitotemporal gyrus.
2. Tau-positive neuronal inclusions were counted in low power microscopic fields: 0, no tau-positive lesions; 1, one neuronal inclusion per few microscopic fields; 2, one inclusion in every field; 3, 4–30 inclusions in every field; 4, over 30 inclusions associated with numerous neurites in every field.
3. Aβ deposits were counted in low power microscopic fields: 0, no Aβ deposits; 1, two to three Aβ plaques in each field; 2, 4–10 Aβ plaques in each field; 3, 11–20 Aβ plaques in each field; 4, more than 20 Aβ deposits in each field.

Hippocampal sclerosis (HS) was defined by neuronal loss with gliosis in the hippocampal CA1 and/or subiculum, with relatively preserved neurons in the CA4, 3, and two regions and absence of intracellular and extracellular NFTs, or ischaemic changes that might explain neuronal loss in the CA1 and subiculum. HS was assessed blind to any clinical or pathological information.

Statistical analysis

The Mann–Whitney *U* test and Fisher's exact test were used to compare the demographic and pathological data between TDP-43-positive and TDP-43-negative groups in PSP and CBD series, respectively. Correlations between ratings of TDP-43 pathology and demographic data, or ratings of tau and Aβ pathologies in each anatomical region were assessed with Spearman's rank-order correlation statistic. Statistical analysis was performed using StatView for Macintosh program, version J-4.5. A value of $p < 0.05$ was accepted as significant.

Confocal laser scanning microscopy

Double-labeling immunofluorescence was performed with the combination of phosphorylation-dependent anti-TDP-43 (pAb pS409/410, rabbit, polyclonal, 1:1,000 [17]) and anti-tau antibodies (AT8, mouse, monoclonal, 1:500, Innogenetics, Ghent, Belgium). Sections from the amygdala and hippocampus in some PSP cases with TDP-43 pathology were pretreated by heating in a microwave oven for 5 min in 10 mM sodium citrate buffer, pH 6.0, at

100°C, allowed to cool then permeabilized with 0.2% (v/v) Triton X-100 in PBS. Following washing in PBS, non-specific antibody binding was blocked with normal sera and sections were incubated with a mixture of the two primary antibodies for 1 h at room temperature. After washing in PBS, sections were incubated with fluorescence-labeled secondary antibodies [AlexaFluor 488 anti-rabbit IgG (1:200) and AlexaFluor 555 anti-mouse IgG (1:200), Molecular Probes, Invitrogen, Paisley. UK]. After washing with PBS, sections were incubated with Toto-3 Iodide (Molecular Probes, Invitrogen, Paisley, UK) with 1 mg/ml RNase (Roche Diagnostics GmbH, Manheim, Germany) at 37°C. To quench (lipofuscin) autofluorescence, sections were incubated in 0.1% Sudan Black B for 10 min at room temperature and washed with 0.1% Tx-PBS for 30 min. Sections were coverslipped with Vectashield mounting media (Vector Laboratories Inc., Burlingame, CA, USA). Images were collected on a Leica TCS SP5 AOBS upright confocal (Leica Microsystems, Milton Keynes, UK) using the 488 nm (19%), 543 nm (30%) and 633 nm (60%) laser lines, respectively. To eliminate cross-talk between channels, the images were collected sequentially.

Immunoblotting

Frozen tissue from the amygdala, hippocampus, and frontal, temporal, and occipital cortices in one PSP case with TDP-43 pathology, one FTLD-TDP case (as a positive control) and eight negative controls (six PSP, one LBD, and one pathologically normal case) were prepared for western blotting according to methods previously described by Neumann et al. [31]. Briefly, 1 g of fresh frozen brain was homogenized in 5 ml/g (w/v) of low salt (LS) buffer-containing 10 mM Tris pH 7.5, 5 mM EDTA pH 8.0, 1 mM DTT, 10% (w/v) sucrose and Roche complete EDTA-free protease inhibitor. Homogenates were sequentially extracted with increasing strength buffers [Triton X-100 buffer (LS buffer + 1% Triton X-100 + 0.5 M NaCl), Triton X-100 buffer with 30% sucrose to float myelin, Sarkosyl buffer (LS buffer + 1% *N*-lauroyl-sarcosine + 0.5 M NaCl)]. Detergent-insoluble pellets were extracted in 0.25 ml/g Urea buffer (7 M Urea, 2 M Thiourea, 4% 3-[(3-Cholamidopropyl) dimethylammonio]-1-propanesulfonate (CHAPS), 30 mM Tris–HCl pH 8.5, Roche complete EDTA free protease inhibitor. Prior to SDS-PAGE immunoblot analysis, urea fractions were added in 1:1 ratio to SDS sample buffer (10 mM Tris pH 6.8, 1 mM EDTA, pH 8.0, 40 mM DTT, 1% SDS, 10% Sucrose, 0.01% Bromophenol Blue). Protein was resolved on 12% Tris–Glycine SDS-PAGE gels along with size standard (Bio-Rad kaleidoscope broad-range marker; Bio-Rad, Hercules, CA, USA). Proteins were transferred onto nitrocellulose membrane (Hybond ECL, GE Life Sciences, UK) and blocked for 1 h at 4°C in 5% (w/v) milk solution [5% powdered milk in Tris-buffered saline containing 0.1% Tween-20 (TBS-T)]. Membranes were incubated in phosphorylation-dependent mouse monoclonal antibody (mAb pS409/410, mouse, 1:1,000 [20]) for 1 h at room temperature followed by HRP-conjugated goat anti-mouse secondary antibody (Santa Cruz Biotechnology Inc, CA, USA). Antibodies were visualized by incubating in enhanced chemiluminescent reagent (ECL, GE Life Sciences) and imaged using the ImageQuant 350 system fitted with a F0,95 25 mm Fixed Lens (GE Healthcare, Life Sciences, UK). TDP-43 probed membranes were exposed for 5 min at different timeframes to obtain multiple images of differing intensity. Images were processed using ImageQuant TL software (GE Healthcare, Life Sciences, UK).

Results

Frequency and distribution of TDP-43 pathology

Clinical and pathological features for all subjects are shown in Table 1. TDP-43 pathology was noted in 5 of 19 PSP cases (26%) and in 2 of 12 CBD cases (17%). Disease duration, gender ratio and brain weight were not statistically different between PSP cases with and without TDP-43 pathology, or between CBD cases with and without TDP-43 pathology, respectively. Age at onset of disease (75 vs. 66 years) and age at death (82 vs. 74 years) tended to be higher, and dementia occurred more often, in PSP cases with TDP-43 pathology than in PSP cases without it (80 vs. 50%), although these differences did not reach statistical significance. One PSP case without TDP-43 pathology also had Lewy body pathology corresponding to brainstem-predominant type [26]. Ten PSP cases (3 TDP-43-positive and 7 TDP-43-negative cases) and four CBD cases (all were TDP-43-negative) had Aβ-positive diffuse plaques in the amygdala, hippocampus, and/or temporal cortex. Of the three TDP-43-positive PSP cases, one case had only a few neuritic plaques in the occipitotemporal gyrus. None of the PSP or CBD cases in our series fit the pathological criteria of AD [9, 28, 39].

In PSP cases, TDP-43-positive NCIs were most frequently noted in the amygdala and dentate gyrus granule cells in the hippocampus (5 cases, 100% of TDP-43-positive PSP cases), followed by the anterior portion of the entorhinal cortex (4 cases, 80%), subiculum (3 cases, 60%), posterior portion of the entorhinal cortex (3 cases, 60%), occipitotemporal gyrus (2 cases, 50%), fusiform gyrus (2 cases, 40%), and CA1 region (2 cases, 20%) (Table 2, Fig. 1a–d). In addition to the rounded inclusions noted in FTLD-TDP, all PSP cases had many irregular shaped

Table 2 Distribution of TDP-43 pathology in PSP and CBD cases

TDP-43 pathology												Hippocampal sclerosis (CA1/Subiculum)	Argyrophilic grains[b]
No.	Amygdala	ant.EC	DG	CA3/4	CA2	CA1	SB	post.EC	FG	OTG	TDP-43 distribution[a]		
PSP cases													
PSP1	++++	−	+	−	−	−	−	−	−	−	Limbic	−	−
PSP2	+++++	+++++	+++++	−	−	−	+	−	−	n	Limbic	+	−
PSP3	+++++	+++++	+++	−	−	−	++	++++	−	−	Limbic	−	−
PSP4	+++++	+++++	++	−	−	+	+++	+++++	+++++	+	Temporal	+	−
PSP5	+++++	+++	+++++	−	−	++	−	++	+++	+++	Temporal	+	Stage III
%	100.0	80.0	100.0	0.0	0.0	20.0	60.0	60.0	40.0	50.0		60.0	20.0
CBD cases													
CBD1	+++	++	−	−	−	−	−	n.a.	n.a.	n.a.	Limbic	−	−
CBD2	+++++	++	++++	++	−	+++++	+++++	++	−	−	Limbic	−	Stage II
%	100.0	100.0	50.0	50.0	0.0	50.0	50.0	50.0	0.0	0.0		0.0	50.0

The stages of TDP-43 pathology: −, no lesion in the anatomical region; +, 1 inclusion in the anatomical region; ++, 2–3 inclusions in the anatomical region; +++, 4–5 inclusion in the anatomical region; ++++, 6–10 inclusions in the anatomical region; +++++, 11 or over inclusions in the anatomical region. The stage of hippocampal sclerosis: −, no; +, mild; ++, moderate; +++, severe. The stage of argyrophilic grains: −, absent; +, present. ant.EC, the anterior portion of the entorhinal cortex; DG, hippocampal dentate gyrus; SB, subiculum; post.EC, the posterior portion of the entorhinal cortex; FG, fusiform gyrus; OTG, occipitotemporal gyrus

[a] The amygdala type: inclusions were present only in the amygdala; the limbic type: inclusions extend to the limbic system, but not in the occipitotemporal gyrus; the temporal type: inclusions are present in the limbic system and occipitotemporal gyrus as well

[b] The distribution of argyrophilic grains are assessed using a staging system proposed by Saito et al. [35]

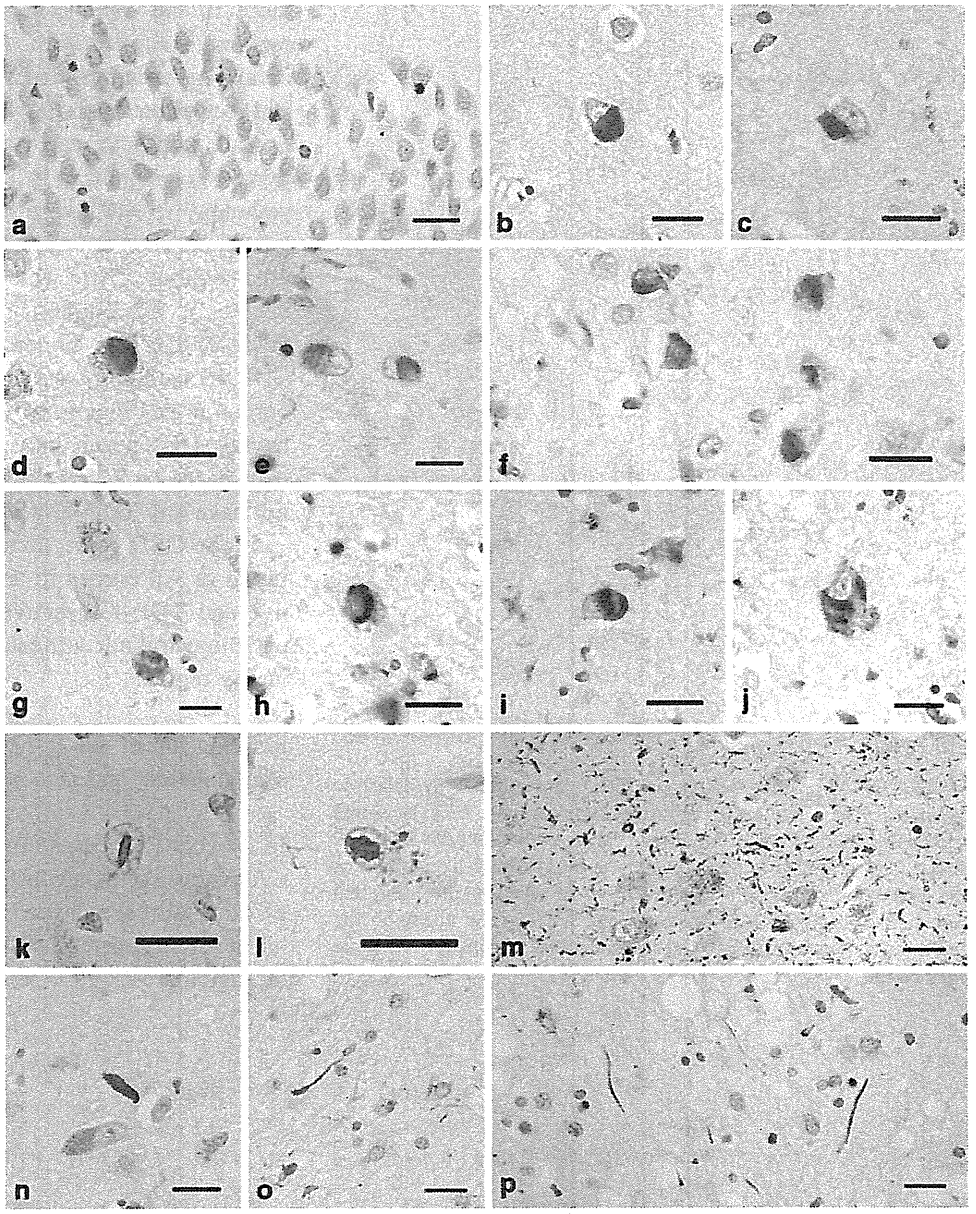

Fig. 1 TDP-43-positive lesions in PSP. **a** Neuronal cytoplasmic inclusions (NCIs) in the hippocampal dentate gyrus. **b–d** NCIs in the entorhinal cortex. Irregular shaped NCIs in the entorhinal cortex (**e**), fusiform gyrus (**f**), and subiculum (**g**). These inclusions have weakly stained or unstained regions. Small dot-like structures are also seen in the neuronal cytoplasm (**g**). Horseshoe-shaped (**h**, **i**) and NFT-like (**j**) NCIs in the entorhinal cortex. Intranuclear inclusions in the amygdala (**k**) and in the subiculum (**l**), cases PSP3 and PSP2, respectively. **m** Massive short threads-like structures in the subiculum, case PSP3. **n** Thick, thread-like structures in the amygdala. **o**, **p** Long, thin thread-like structures in the amygdala. pAb pS409/410 immunohistochemistry. All *scale bars* 20 μm

NCIs, such as flame-shape NFT-like, globose-type NFT-like, and horseshoe-like inclusions (Fig. 1e–j). One PSP case (PSP 2 in Table 2) showed a few NII in the subiculum (Fig. 1k, l). Two cases (PSP4 and PSP5) had abundant fine, short, thread-like structures immunopositive for TDP-43 from the CA1 to subiculum (Fig. 1m). TDP-43-positive thread-like structures were also observed in the amygdala (3 cases), entorhinal cortex (2 cases), CA1 (one case), and subiculum (one case) (Fig. 1n–p).

In two CBD cases, TDP-43-positive NCIs were observed in the amygdala, entorhinal cortex, hippocampal dentate gyrus, CA1, CA3/4, and subiculum (Table 2, Fig. 2a). The distribution of TDP-43 pathology was roughly consistent with that observed in PSP cases. NIIs were found in the subiculum and amygdala in one CBD case with severe TDP-43 pathology (Fig. 2b, c). Short thread-like structures immunopositive for TDP-43 were found in the amygdala, entorhinal cortex, CA1, CA3, and/or subiculum in both CBD cases with TDP-43 pathology. One CBD case had TDP-43-positive coiled body-like structures and thread-like structures in the alveus in the subiculum (Fig. 2d–f). Abnormal accumulation of TDP-43 was not found in the white matter of the temporal lobe and substantia nigra in any of the TDP-43-positive PSP or CBD cases.

Relationship between TDP-43 pathology and tau or Aβ burden

The ratings for tau burden in the TDP-43-positive PSP cases tended to be higher (but not significantly so) than

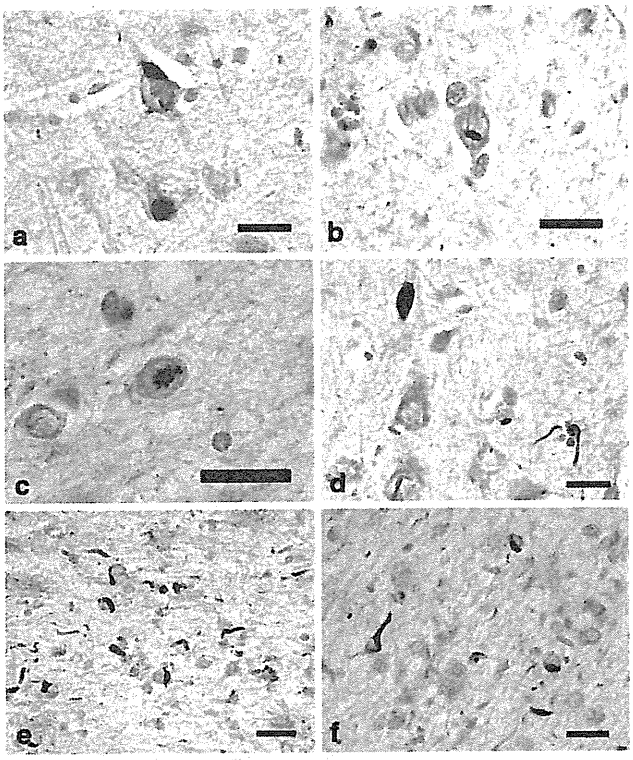

Fig. 2 TDP-43-positive lesions in CBD. **a** Neuronal cytoplasmic inclusions (NCIs) in CA3 region of hippocampus. **b**, **c** Neuronal intranuclear inclusions in the amygdala. **d** A thick neurite and thin, thread-like structures in the amygdala. **e** Short thread-like structures and glial cytoplasmic inclusions (GCIs) in the alveus in the entorhinal cortex. **f** Coiled body-like structures and GCis in the alveus in the entorhinal cortex. pAb pS409/410 immunohistochemistry. All *scale bars* 20 μm

those in the TDP-43-negative PSP cases, in almost all regions examined (i.e., including amygdala, entorhinal cortex, hippocampal dentate gyrus, CA1-4, fusiform gyrus, and occipitotemporal gyrus) (Fig. 3). In the PSP cases overall, rating for tau pathology in the occipitotemporal gyrus was significantly correlated with that of TDP-43 pathology ($r = 0.504$, $p < 0.05$), but no significant correlations between tau and TDP-43 ratings were found in any other regions. There were no significant differences in the degree of Aβ burden in any region between TDP-43-positive and TDP-43-negative PSP cases, and ratings for TDP-43 pathology did not correlate with those for Aβ burden in any region. Of three TDP-43-positive PSP cases having Aβ deposits, only one case had a few neuritic plaques in the occipitotemporal gyrus; however, this case did not have any TDP-43-positive inclusions in the region.

In the CBD cases, there were no significant differences in tau or Aβ burden in any region between TDP-43-positive and TDP-43-negative cases, and ratings for TDP-43 pathology did not correlate with those for tau or Aβ burden in any region.

Relationship of HS, argyrophilic grains, TDP-43 accumulation, and dementia

In 3 of 19 PSP cases (16%), evident neuronal loss in the CA1 and subiculum consistent with HS was noted (Fig. 4a, b). No CBD case showed HS. All three PSP cases with HS had a various degrees of TDP-43 pathology in the CA1 and/or subiculum (Fig. 4e–h), and two had extensive TDP-43

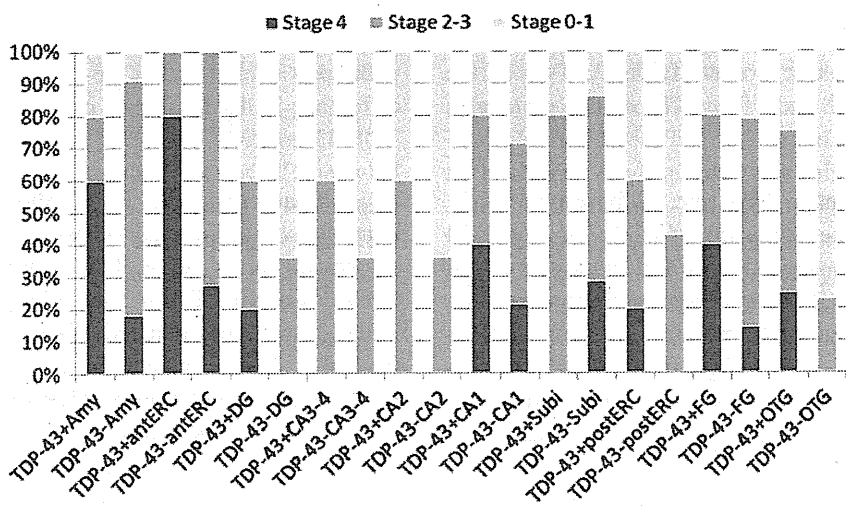

Fig. 3 Tau burden in the limbic system in PSP cases with and without TDP-43 pathology. In all regions but the subiculum, tau burden in PSP cases with TDP-43 pathology is more severe than that in PSP cases without TDP-43 pathology. Stage 0–1, no to mild tau deposition; stages 2–3, moderate to severe tau deposition; stage 4, very severe tau deposition (see detailed definition in the text). *TDP-43+* TDP-43-positive, *TDP-43−* TDP-43-negative, *Amy* amygdala, *antERC* the anterior portion of the entorhinal cortex, *DG* hippocampal dentate gyrus, *Subi* subiculum, *postERC* the posterior portion of the entorhinal cortex, *FG* fusiform gyrus, *OTG* occipitotemporal gyrus

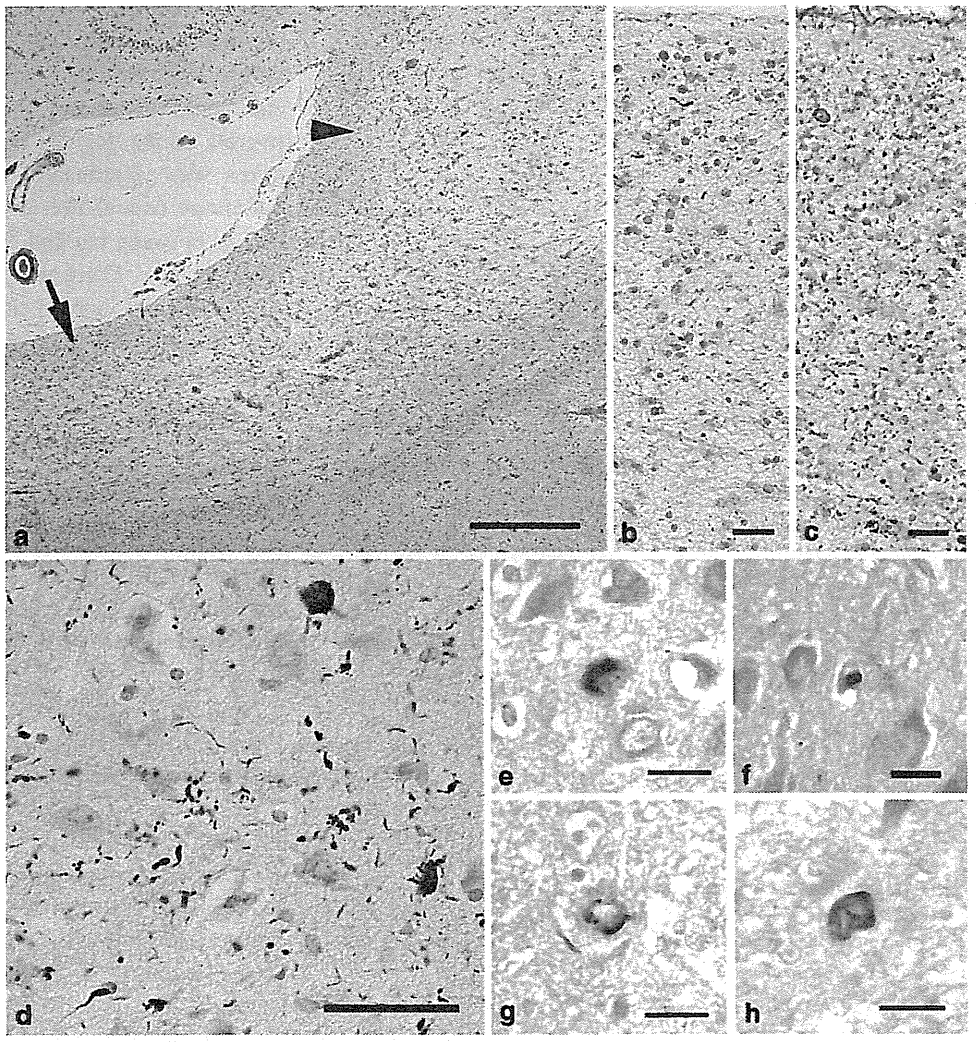

Fig. 4 Pathological features in the hippocampus in a PSP case with TDP-43, HS, and argyrophilic grains (PSP5). **a** A low power view of the hippocampal CA1 to subiculum. Severe reduction of the width with tissue rarefaction is noted in the subiculum (*arrow*) and to a lesser degree in the adjacent CA1 region (*arrowhead*). **b** A moderate power view of the subiculum on the same section as that shown in **a**. Severe neuronal loss associated with gliosis is evident. Argyrophilic threads and grains are scattered, but tangles are rare. **c** The subiculum on an adjacent section of **b**. A moderate number of tau-positive threads and grains, but only a few tangles, are seen. **d** Argyrophilic grains in CA1 region. **e**, **f** TDP-43-positive cytoplasmic inclusions in CA1 region. **g** An irregular shaped TDP-43 accumulation in the subiculum. **h** A coiled body-like TDP-43-positive inclusion in the subiculum. **a**, **b**, **d** Gallyas-Braak hematoxylin-eosin stain. **c** AT-8 immunohistochemistry. **e**–**h** pAb pS409/410 immunohistochemistry. *Scale bars* **a** 400 μm, **b**, **c** 25 μm, **d** 50 μm, **e**–**h** 20 μm

pathology in the limbic system: one case had both TDP-43 pathology and argyrophilic grains (Table 2). Two of the three PSP cases with HS had a few AT8-positive pretangles and argyrophilic grains in the CA1 and subiculum (Fig. 4b–d). Neurofibrillary tangles were rare in these regions in all PSP cases with HS (Fig. 4b). No significant ischemic changes in the hippocampal pyramidal neurons, or neuronal loss in the end plate, suggestive of a past history of severe epilepsy was noted in any of the PSP cases with HS. The frequency of HS in the TDP-43-positive PSP cases was significantly higher than that in TDP-43-negative PSP cases (60 vs. 0%, $p = 0.021$). Dementia was present in all of the 3 TDP-43-positive PSP cases with HS (100%), 4 of the 5 TDP-43-positive PSP cases with and without HS (80%), 1 of 2 TDP-43-positive PSP cases without HS (50%), and 7 of 14 PSP cases lacking both (50%). The frequency of dementia was not significantly different between PSP cases with and without HS ($p = 0.170$).

Concomitant argyrophilic grains were observed in four PSP (21%) and three CBD cases (25%) (Fig. 4d). Among these cases, one PSP and one CBD case had TDP-43 pathology (Table 2, Fig. 4e–h). There was no significant difference in the frequency of argyrophilic grains between TDP-43-positive and TDP-43-negative PSP cases, or between CBD cases with and without TDP-43 pathology, respectively. However, in the TDP-43-positive PSP and CBD cases, argyrophilic grains were found in those cases with the most severe TDP-43 pathology (Table 2).

Double immunofluorescence labeling in PSP cases

In the PSP cases examined, TDP-43 and tau pathologies were independently present in the perikarya of granular cells in the hippocampal dentate gyrus with no coexistence of these proteins (Fig. 5a–f). In contrast, in the amygdala, TDP-43 accumulation was often intermingled with tau accumulation in NCIs and dystrophic neurites, and colocalization was frequent (Fig. 5g–o). In the entorhinal cortex and parahippocampal gyrus in one PSP case with argyrophilic grains, many tau-positive grain-like structures

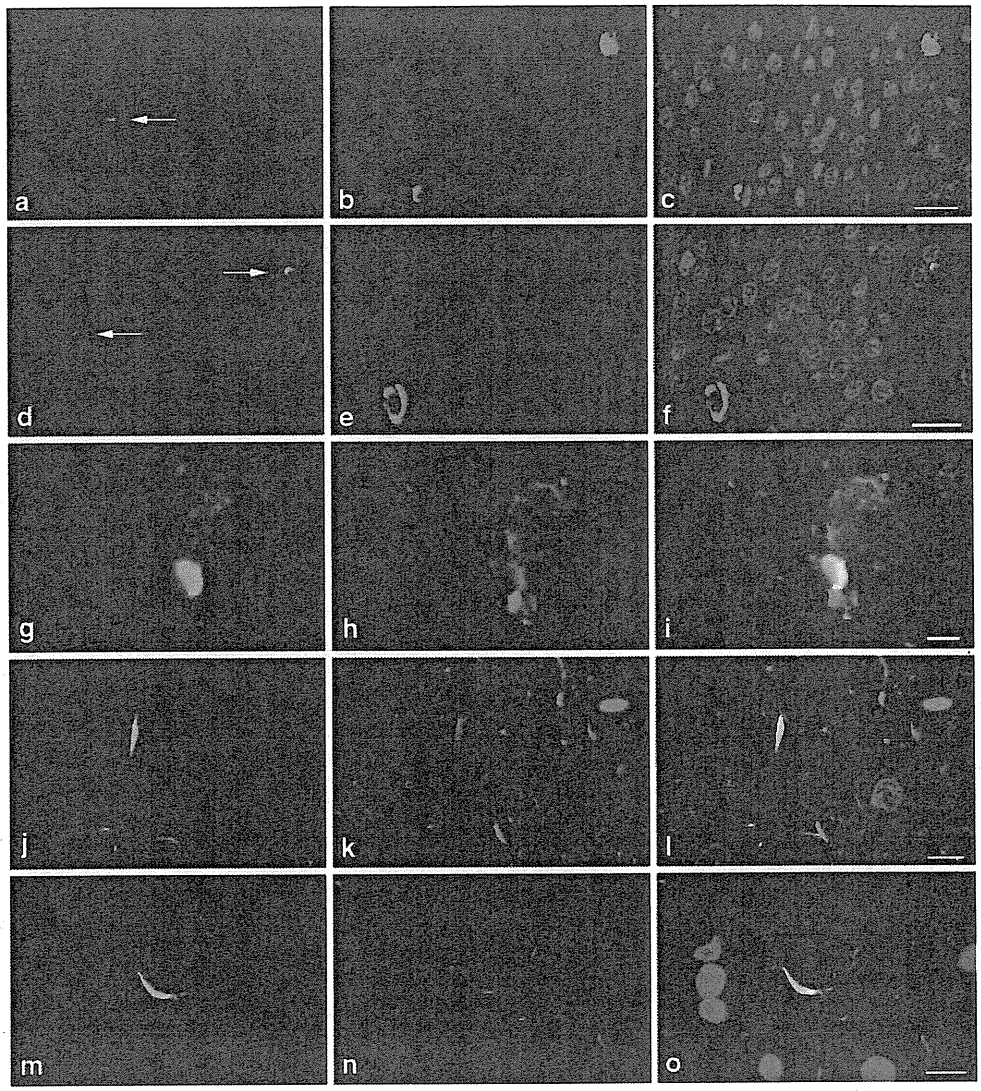

Fig. 5 Confocal double-imunofluorescence of TDP-43 (**a**, **d**, **g**, **j**, **m**) and tau (**b**, **e**, **h**, **k**, **n**) in PSP cases. *Merged images* are shown in **c**, **f**, **i**, **l**, and **o**. Blue fluorescence in merged images are nuclei. **a–f** In the hippocampal dentate gyrus, TDP-43 accumulation (*arrows*) is not colocalized with tau labeling. **g–i** In the amygdala, TDP-43 accumulation is often intermingled and colocalized with neuronal tau accumulation. **j–o** TDP-43-positive neurites (**j**, **m**) and many tau-positive neurites and granules (**k**, **n**) are seen in the amygdala. Coexistence of TDP-43 and tau is noted in some neurites (**l**, **o**). AT8 and pAb pS409/410 double immunofluorescence. *Scale bars* **a–c** 25 μm, **d–f** 25 μm, **g–i** 2.5 μm, **j–l** 7.5 μm, **m–o** 7.5 μm

were demonstrated, and TDP-43 was colocalized with tau in some of these structures (data not shown).

Biochemical analyses of TDP-43 in PSP cases

Immunoblot analysis of the sarkosyl-insoluble, urea-soluble fraction with mAb pS409/410 demonstrated distinct bands at (approximately) 45 and 25 kDa, as well as high molecular weight smears in the amygdala of a PSP case having TDP-43 pathology (Fig. 6, lane 6) and in the frontal cortex of a FTLD-TDP case (lane 5). Weak 25 and 45 kDa bands were also observed in the hippocampus in a PSP case, which had very mild TDP-43 pathology at this site (lane 7). Pathological TDP-43 bands and smear were not demonstrated in any of the other cases lacking TDP-43 pathology, including those with PSP (lanes 1 and 2) or Lewy body disease (lane 4), or in normal control cases (lane 3).

Discussion

This is the first study demonstrating abnormal accumulations of phosphorylated TDP-43 in the limbic system in a significant proportion (26%) of patients with PSP. Immunoblot analysis also demonstrated biochemical alterations in TDP-43 in tissue samples from a PSP case with TDP-43 pathology, similar to those in FTLD-TDP and ALS. Regional tau burden in PSP cases with TDP-43 pathology was higher than that in PSP cases without it, and TDP-43 burden was significantly correlated with that of tau in the occipitotemporal cortex. The frequency of HS in PSP cases with TDP-43 pathology was significantly higher than that in PSP cases without it. Collectively, these findings suggest that (1) PSP is one of the tauopathies in which pathological TDP-43 accumulation can occur in the limbic system, and (2) TDP-43 pathology may be associated with the occurrence of HS in PSP cases.

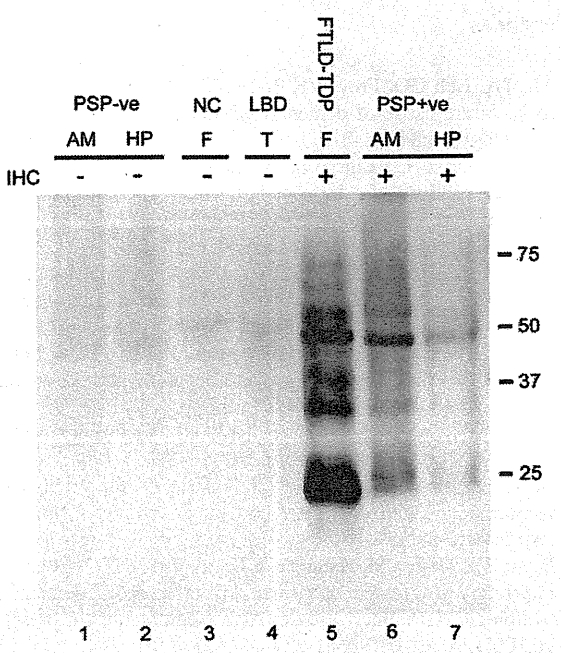

Fig. 6 Immunoblot analysis of the sarkosyl-insoluble fraction in representative PSP cases with phosphorylation-dependent monoclonal anti-TDP-43 antibody (mAb pS409/410). The 45 kDa full length TDP-43, 25 kDa fragments, and high molecular weight smear are strongly labeled in the amygdala of a PSP case with TDP-43 pathology (*lane 6*) and in the frontal cortex of a FTLD-TDP case (*lane 5*). Weakly stained 45 and 25 kDa bands are noted in the hippocampus of a PSP case (*lane 7*), in which TDP-43 pathology was mild. Similar 45 and 25 kDa bands and smears were not immunolabeled in any of the other cases without detectable TDP-43 pathology by immunohistochemistry (*lanes 1–4*). Normal 43 kDa TDP-43 is not stained by this phophorylation-dependent antibody in any case. *PSP* progressive supranuclear palsy, *LBD* Lewy body disease, *NC* normal control, *AM* amygdala, *HP* hippocampus, *F* frontal cortex, *T* temporal cortex, *IHC* pAb pS409/410 immunohistochemistry

Previous studies have demonstrated variable frequencies of concurrent TDP-43 pathology in many tauopathies: 23–56% in AD cases [2, 4, 40], 31–60% in DLB + AD cases [4, 30], 15% in CBD cases [40], and 60% in AGD cases [14]. Why no cases of PSP with TDP-43 pathology have previously been described is not clear. Our present findings show that, at least some, PSP cases may share a common pathophysiological background involving TDP-43 accumulation with other tauopathies with TDP-43 pathology. Several studies demonstrated that concurrent AD-type pathology was associated with the development of TDP-43 pathology in some neurodegenerative diseases [2, 4, 7, 14, 30]. However, it was unlikely that the development of TDP-43 pathology in our PSP series can be explained by the influence of Aβ deposits or neuritic plaques. For example, of all ten PSP cases having Aβ deposits, nine cases had only diffuse plaques, and the degree of Aβ deposition was not significantly different between TDP-43-positive and TDP-43-negative PSP cases and was not correlated with that of TDP-43 pathology in any regions. Although only one PSP case had a few neuritic plaques in the occipitotemporal gyrus, no TDP-43-positive inclusion was noted in the region.

Our findings are inconsistent with previous studies that failed to demonstrate immunohistochemical or biochemical abnormalities of TDP-43 in PSP cases [2, 3, 18, 40]. Considering that the sample size investigated in one of these previous studies [40] was far larger than that in our own study, the most plausible cause of the discrepancy may be the difference of the sensitivities of anti-TDP-43 antibodies employed: phosphorylation-dependent anti-TDP-43 antibodies do not stain normal nuclei, making true TDP-43-positive inclusions more readily identifiable [17, 37]. The distribution of TDP-43 pathology observed in our PSP cases was very similar to that reported previously in AD [2, 4, 18, 19, 40], DLB + AD [4, 30], and CBD [40], but tended to be more restricted than that in ALS/PDC of Guam [15, 16, 27]. Most frequently affected sites in these tauopathies are the amygdala and hippocampal dentate gyrus. Given these findings, it is plausible that the frequent TDP-43 accumulation in these sites in tauopathies is associated with some region-specific, rather than disease-specific, mechanism. On the other hand, it remains unclear whether TDP-43 is abnormally accumulated through an identical pathophysiological mechanism in various anatomical regions. For example, it was reported that abnormal TDP-43 accumulation was significantly correlated with the severity of tau pathology in AD cases [4] and Lewy body disease including many DLB + AD cases [30]. This same statistical relationship was observed in our PSP cases. Furthermore, in our present studies, TDP-43 was often colocalized with tau in NCIs and dystrophic neurites in the amygdala, although there were also TDP-43-positive but tau-negative lesions in this site. A coexistence of TDP-43 and tau in the same neuron in the amygdala and temporal cortex was also reported in AD and DLB cases in previous studies [4, 18]. However, in contrast to the amygdala, a coexistence of TDP-43 and tau in the same neuron in the hippocampal dentate gyrus was not seen in our PSP cases. This trend regarding non-colocalization of these two proteins was also noticed in the dentate granular cells in AD [40] and AGD brains [14]. This suggests that the mechanism underlying the accumulation of TDP-43 is different at least between the amygdala and hippocampal dentate gyrus, or that there is some unknown factor that can influence the occurrence of both TDP-43 and tau pathologies. In addition, considering the potential relationship between tau and TDP-43 in PSP presented in this paper, whether TDP-43 pathology is also noted in several other regions that are often involved by tau-associated lesions (e.g., the frontal cortex and basal ganglia) needs to be investigated in the future studies.

There is little known about the relationship between PSP and HS. In our series, 3 of 19 PSP cases (16%) had evident neuronal loss in the CA1 and/or subiculum consistent with the definition of HS. Furthermore, all of the cases with HS had TDP-43 pathology, and one of the three cases also had argyrophilic grains. It has been reported that HS cases have variable underling pathologies, including the 'pure form' of HS [1, 21, 34], FTLD-TDP [23], FTLD with motor neuron disease [29], AD [2], CBD [36], DLB [13], and AGD [5, 13]. Present findings support the possibility that the development of HS, at least in some PSP cases, may occur in association with concurrent TDP-43 pathology. On the other hand, whether the development of HS in PSP cases is correlated with the severity of tau or TDP-43 pathology remains unclear. Considering the relatively small size of the samples examined in the present study, the relationship between HS and TDP-43 accumulation in PSP, as well as the frequencies of these pathological features, needs to be confirmed in a larger case series.

Although influence of concurrent TDP-43 pathology on clinical features in tauopathies is not fully understood, some previous studies in AD, have demonstrated a comorbidity such that a concomitant TDP-43 pathology was associated with a later age at onset and death [4, 24], and significantly poorer cognitive function [24]. On the other hand, a study investigating a relatively small series of AGD did not demonstrate any significant difference in the age at death or disease duration between cases with and without TDP-43 pathology [14]. It is known that patients with PSP frequently exhibit psychiatric and behavioral disturbances, and that cognitive decline in PSP is associated with the atrophy in the orbitofrontal cortex [11] and more severe tau burden in the neocortex and hippocampus [6, 8, 22]. More recently, it was also reported that clinical presentation, including the occurrence of dementia, is influenced by the distribution and severity of tau pathology [42, 43]. In our PSP series, although not statistically significantly, the frequency of dementia in PSP cases with both TDP-43 and HS (100%), and that in all PSP cases with TDP-43 pathology (80%), were higher than that in PSP cases lacking both (50%). The potential co-morbid effect of concurrent TDP-43 pathology and/or HS on cognitive impairment in patients with PSP needs to be explored by further clinicopathological studies.

Acknowledgments This study was supported in part by a research grant from the Uehara Memorial Foundation and Grant No. AG13854 from the National Institutes of Health. We thank Ms. M. Onbe (Department of Neuropsychiatry. Okayama University Graduate School of Medicine, Dentistry and Pharmaceutical Sciences) for their excellent technical assistance, and the Parkinson's Disease Society Brain Bank for making available tissue samples for this study. A part of this study was presented at the 111th annual meeting of the British Neuropathological Society in January 2010.

References

1. Ala TA, Beh GO, Frey WH 2nd (2000) Pure hippocampal sclerosis: a rare cause of dementia mimicking Alzheimer's disease. Neurology 54:843–848
2. Amador-Ortiz C, Lin WL, Ahmed Z et al (2007) TDP-43 immunoreactivity in hippocampal sclerosis and Alzheimer's disease. Ann Neurol 61:435–445
3. Arai T, Hasegawa M, Akiyama H et al (2006) TDP-43 is a component of ubiquitin-positive tau-negative inclusions in frontotemporal lobar degeneration and amyotrophic lateral sclerosis. Biochem Biophys Res Commun 351:602–611
4. Arai T, Mackenzie IR, Hasegawa M et al (2009) Phosphorylated TDP-43 in Alzheimer's disease and dementia with Lewy bodies. Acta Neuropathol 117:125–136
5. Beach TG, Sue L, Scott S et al (2003) Hippocampal sclerosis dementia with tauopathy. Brain Pathol 13:263–278
6. Bigio EH, Brown DF, White CL 3rd (1999) Progressive supranuclear palsy with dementia: cortical pathology. J Neuropathol Exp Neurol 58:359–364
7. Bigio EH, Mishra M, Hatanpaa KJ et al (2010) TDP-43 pathology in primary progressive aphasia and frontotemporal dementia with pathologic Alzheimer disease. Acta Neuropathol (in press). doi: 10.1007/s00401-010-0681-2
8. Braak H, Braak E (1990) Neurofibrillary changes confined to the entorhinal region and an abundance of cortical amyloid in cases of presenile and senile dementia. Acta Neuropathol 80:479–486
9. Braak H, Alafuzoff I, Arzberger T, Kretzschmar H, Del Tredici K (2006) Staging of Alzheimer disease-associated neurofibrillary pathology using paraffin sections and immunocytochemistry. Acta Neuropathol 112:389–404
10. Cairns NJ, Neumann M, Bigio EH et al (2007) TDP-43 in familial and sporadic frontotemporal lobar degeneration with ubiquitin inclusions. Am J Pathol 171:227–240
11. Cordato NJ, Duggins AJ, Halliday GM, Morris JG, Pantelis C (2005) Clinical deficits correlate with regional cerebral atrophy in progressive supranuclear palsy. Brain 128:1259–1266
12. Davidson Y, Kelley T, Mackenzie IR et al (2007) Ubiquitinated pathological lesions in frontotemporal lobar degeneration contain the TAR DNA-binding protein, TDP-43. Acta Neuropathol 113:521–533
13. Dickson DW, Davies P, Bevona C et al (1994) Hippocampal sclerosis: a common pathological feature of dementia in very old (> or = 80 years of age) humans. Acta Neuropathol 88:212–221
14. Fujishiro H, Uchikado H, Arai T et al (2009) Accumulation of phosphorylated TDP-43 in brains of patients with argyrophilic grain disease. Acta Neuropathol 117:151–158
15. Geser F, Winton MJ, Kwong LK et al (2008) Pathological TDP-43 in parkinsonism-dementia complex and amyotrophic lateral sclerosis of Guam. Acta Neuropathol 115:133–145
16. Hasegawa M, Arai T, Akiyama H et al (2007) TDP-43 is deposited in the Guam parkinsonism-dementia complex brains. Brain 130:1386–1394
17. Hasegawa M, Arai T, Nonaka T et al (2008) Phosphorylated TDP-43 in frontotemporal lobar degeneration and amyotrophic lateral sclerosis. Ann Neurol 64:60–70
18. Higashi S, Iseki E, Yamamoto R et al (2007) Concurrence of TDP-43, tau and alpha-synuclein pathology in brains of Alzheimer's disease and dementia with Lewy bodies. Brain Res 1184:284–294
19. Hu WT, Josephs KA, Knopman DS et al (2008) Temporal lobar predominance of TDP-43 neuronal cytoplasmic inclusions in Alzheimer disease. Acta Neuropathol 116:215–220

20. Inukai Y, Nonaka T, Arai T et al (2008) Abnormal phosphorylation of Ser409/410 of TDP-43 in FTLD-U and ALS. FEBS Lett 582:2899–2904
21. Jellinger KA (2000) Pure hippocampal sclerosis: a rare cause of dementia mimicking Alzheimer's disease. Neurology 55:739–740
22. Jellinger KA (2008) Different tau pathology pattern in two clinical phenotypes of progressive supranuclear palsy. Neurodegener Dis 5:339–346
23. Josephs KA, Dickson DW (2007) Hippocampal sclerosis in tau-negative frontotemporal lobar degeneration. Neurobiol Aging 28:1718–1722
24. Josephs KA, Whitwell JL, Knopman DS et al (2008) Abnormal TDP-43 immunoreactivity in AD modifies clinicopathologic and radiologic phenotype. Neurology 70:1850–1857
25. Kabashi E, Valdmanis PN, Dion P et al (2008) TARDBP mutations in individuals with sporadic and familial amyotrophic lateral sclerosis. Nat Genet 40:572–574
26. McKeith IG, Dickson DW, Lowe J et al (2005) Diagnosis and management of dementia with Lewy bodies: third report of the DLB Consortium. Neurology 65:1863–1872
27. Miklossy J, Steele JC, Yu S et al (2008) Enduring involvement of tau, β-amyloid, α-synuclein, ubiquitin and TDP-43 pathology in the amyotrophic lateral sclerosis/parkinsonism–dementia complex of Guam (ALS/PDC). Acta Neuropathol 116:625–637
28. Mirra SS, Heyman A, McKeel D et al (1991) The Consortium to Establish a Registry for Alzheimer's Disease (CERAD). Part II. Standardization of the neuropathologic assessment of Alzheimer's disease. Neurology 41:479–486
29. Nakano I (1993) Temporal lobe lesions in amyotrophic lateral sclerosis with or without dementia—a neuropathological study. Neuropathology 13:215–227
30. Nakashima-Yasuda H, Uryu K et al (2007) Co-morbidity of TDP-43 proteinopathy in Lewy body related diseases. Acta Neuropathol 114:221–229
31. Neumann M, Sampathu DM, Kwong LK et al (2006) Ubiquitinated TDP-43 in frontotemporal lobar degeneration and amyotrophic lateral sclerosis. Science 314:130–133
32. Neumann M, Mackenzie IR, Cairns NJ et al (2007) TDP-43 in the ubiquitin pathology of frontotemporal dementia with VCP gene mutations. J Neuropathol Exp Neurol 66:152–157
33. Obi K, Akiyama H, Kondo H et al (2008) Relationship of phosphorylated alpha-synuclein and tau accumulation to Abeta deposition in the cerebral cortex of dementia with Lewy bodies. Exp Neurol 210:409–420
34. Probst A, Taylor KI, Tolnay M (2007) Hippocampal sclerosis dementia: a reappraisal. Acta Neuropathol 114:335–345
35. Saito Y, Ruberu NN, Sawabe M et al (2004) Staging of argyrophilic grains: an age-associated tauopathy. J Neuropathol Exp Neurol 63:911–918
36. Schneider JA, Watts RL, Gearing M et al (1997) Corticobasal degeneration: neuropathologic and clinical heterogeneity. Neurology 48:959–969
37. Schwab C, Arai T, Hasegawa M, Yu S, McGeer PL (2008) Colocalization of transactivation-responsive DNA-binding protein 43 and huntingtin in inclusions of Huntington disease. J Neuropathol Exp Neurol 67:1159–1165
38. Sreedharan J, Blair IP, Tripathi VB et al (2008) TDP-43 mutations in familial and sporadic amyotrophic lateral sclerosis. Science 319:1668–1672
39. The National Institute on Aging, and Reagan Institute Working Group (1997) Consensus recommendations for the postmortem diagnosis of Alzheimer disease. The National Institute on Aging, and Reagan Institute Working Group on diagnostic criteria for the neuropathological assessment of Alzheimer disease. Neurobiol Aging 18:S1–S2
40. Uryu K, Nakashima-Yasuda H, Forman MS et al (2008) Concomitant TAR-DNA-binding protein 43 pathology is present in Alzheimer disease and corticobasal degeneration but not in other tauopathies. J Neuropathol Exp Neurol 67:555–564
41. Van Deerlin VM, Leverenz JB, Bekris LM et al (2008) TARDBP mutations in amyotrophic lateral sclerosis with TDP-43 neuropathology: a genetic and histopathological analysis. Lancet Neurol 7:409–416
42. Williams DR, Lees AJ (2009) Progressive supranuclear palsy: clinicopathological concepts and diagnostic challenges. Lancet Neurol 8:270–279
43. Williams DR, Holton JL, Strand C et al (2007) Pathological tau burden and distribution distinguishes progressive supranuclear palsy-parkinsonism from Richardson's syndrome. Brain 130:1566–1576
44. Yokoseki A, Shiga A, Tan CF et al (2008) TDP-43 mutation in familial amyotrophic lateral sclerosis. Ann Neurol 63:538–542

INTERNAL MEDICINE

CASE REPORT

TDP-43 M337V Mutation in Familial Amyotrophic Lateral Sclerosis in Japan

Akira Tamaoka[1], Makoto Arai[2], Masanari Itokawa[2], Tetsuaki Arai[2], Masato Hasegawa[2], Kuniaki Tsuchiya[3], Hiroshi Takuma[1], Hiroshi Tsuji[1], Akiko Ishii[1], Masahiko Watanabe[1], Yuji Takahashi[4], Jun Goto[4], Shoji Tsuji[4] and Haruhiko Akiyama[2]

Abstract

The clinical features of a Japanese family with autosomal dominant adult-onset amyotrophic lateral sclerosis (ALS) are reported. Weakness initially affected the bulbar musculature, with later involvement of the extremities. Genetic studies failed to detect any mutations of the Cu/Zn superoxide dismutase-1 (SOD1) and Dynactin1 (DCTN1) genes, but revealed a single base pair change from wild-type adenine to guanine at position 1009 in TAR-DNA-binding protein (TDP-43), resulting in a methionine-to-valine substitution at position 337. The immunohistochemical study on autopsied brain of the proband's aunt showed TDP-43-positive cytoplasmic inclusions in the anterior horn cells of the spinal cord and in the hypoglossal nucleus, as well as glial cytoplasmic inclusions in the precentral gyrus, suggesting that a neuroglial proteinopathy was related to TDP-43. In conclusion, a characteristic clinical phenotype of familial ALS with initial bulbar symptoms occurred in this family with TDP-43 M337V substitution, the pathomechanism of which should be elucidated.

Key words: Amyotrophic lateral sclerosis (ALS), TAR-DNA-binding protein 43 (TDP-43)

(Inter Med 49: 331-334, 2010)
(DOI: 10.2169/internalmedicine.49.2915)

Introduction

Amyotrophic lateral sclerosis (ALS) is a progressive and fatal neurodegenerative disorder that is characterized pathologically by the degeneration of motor neurons in the brain and spinal cord, and clinically by progressive weakness and death within a few years of onset. Recently, TAR DNA-binding protein 43 (TDP-43) was identified as the major pathological protein in the motor neuron inclusions found in sporadic ALS and superoxide dismutase 1 (SOD1)-negative familial ALS, as well as in frontotemporal lobar degeneration with ubiquitin-immunoreactive, tau-negative inclusions (FTLD-U). Although the role of TDP-43 in the pathogenesis of these neurodegenerative disorders remains to be elucidated, several mutations of TDP-43 have been identified in individuals with sporadic and familial ALS, suggesting that TDP-43 may be a causative protein for these disorders (1-6). Here we first report the detailed clinical features of affected members of a Japanese family who suffered from ALS linked to TDP-43 M337V mutation.

Case Report

The proband (III-2 in Fig. 1-1) was a Japanese woman aged 61 years. She developed dysarthria at the age of 55 years, which became progressively worse. One year later, she also noted dysphagia. Neurological examination at the age of 56 revealed minimal atrophy of the facial muscles and tongue, markedly diminished reflexes of the palatal and pharyngeal muscles, and slow movements and minimal fasciculation of the tongue. Her deep tendon reflexes, including the jaw jerk, were highly exaggerated. At the age of 57, her dysphagia worsened, and atrophy and fasciculation of the

[1]Department of Neurology, Doctoral Program in Medical Sciences for Control of Pathological Processes, Graduate School of Comprehensive Human Sciences, University of Tsukuba, Tsukuba, [2]Tokyo Institute of Psychiatry, Tokyo, [3]Tokyo Metropolitan Matsuzawa Hospital, Tokyo and [4]Department of Neurology, Graduate School of Medicine, University of Tokyo, Tokyo
Received for publication September 18, 2009; Accepted for publication October 18, 2009
Correspondence to Dr. Akira Tamaoka, atamaoka@md.tsukuba.ac.jp

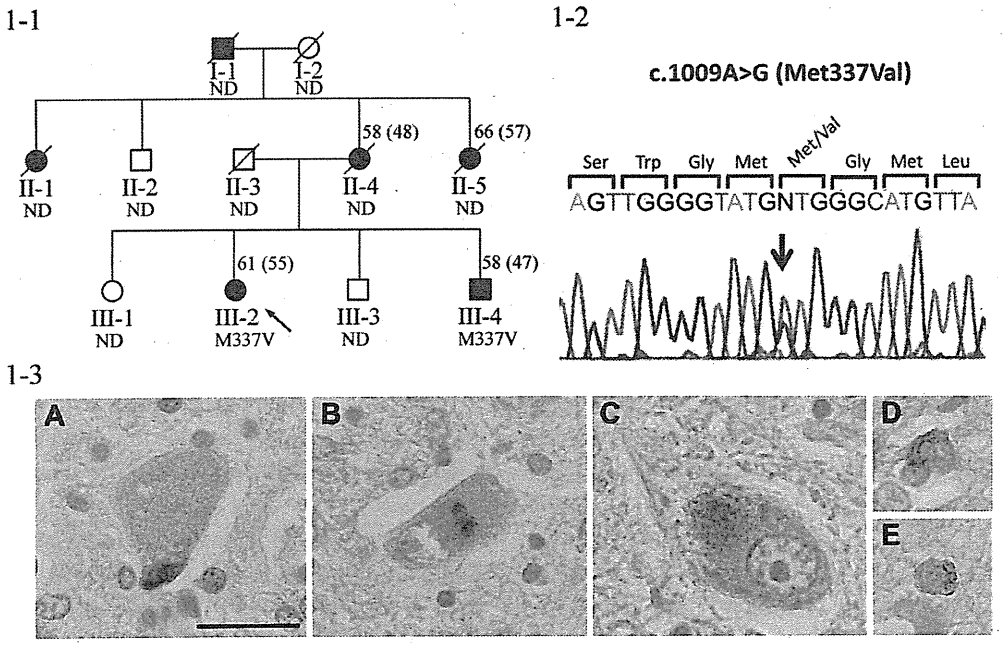

Figure 1. 1-1. Pedigree of the present family. Circles represent women and squares represent men. The slashed symbols indicate deceased subjects. Known affected persons are shown as filled symbols. The arrow represents the proband. Age at death or current age and age at disease onset in parenthesis are indicated. ND=not determined. 1-2. Chromatogram of Patient III-2 (the proband). Chromatogram shows the heterozygous sequence trace of A to G for genotyping by the reverse primer. The nucleotide position of substitution is indicated by arrow. 1-3. Immunocytochemical findings in Patient II-5. TDP-43 positive cytoplasmic inclusions in the anterior horn of the spinal cord (A, B) and in the hypoglossal nucleus (C). Glial cytoplasmic inclusions in the precentral gyrus (D, E). (A, C) Phosphorylation-independent anti-TDP-43 antibody; (B, D, E) phosphorylation-dependent anti-TDP-43 antibody (pS409/410). The sections were counterstained with hematoxylin to reveal nuclei. Bar in A=25 μm.

tongue became more prominent. Muscle weakness of the lower extremities showed slow progression, predominantly in the distal regions. At the age of 58, she was almost unable to protrude her tongue. At the age of 61, she also noted mild weakness of the upper extremities. Needle EMG showed marked neurogenic changes of the biceps, abducens pollicis brevis, vastus lateralis and tibialis anterior muscles of the right side, as well as a mild neurogenic pattern in her right masseter.

The aunt of the proband (II-5 in Fig. 1-1), a Japanese woman, developed dysarthria at the age of 57 years, followed by dysphagia, weakness of the upper extremities, and difficulty with breathing. She could walk without support until her death at the age of 66. The results of the neuropathological examination were reported in detail (7).

The younger brother of the proband (III-4 in Fig. 1-1), a Japanese man, developed dysarthiria at the age of 44 years. Neurological examination at the age of 47 showed slight dysarthria, poor movement of the soft palate, exaggerated pharyngeal reflexes and jaw jerk, slow movements, slight atrophy and fasciculation of the tongue. These findings were mainly related to pseudobulbar palsy. He also showed hyperreflexia in the upper and lower extremities (predominantly in the latter) without any pathological reflexes. Needle EMG revealed neurogenic changes of the masseter and orbicularis oris muscles, while there was a normal pattern in the tongue and extremities. He had no dysphagia, muscle weakness, or atrophy of the upper and lower extremities, as well as no sensory disturbance or vesicorectal disturbance. He could stand and walk unaided. His condition deteriorated slowly and progressively over the next 10 years. At present, he is 58 years old and virtually bed-ridden with a gastrostomy and minimal communication. Patient II-4, Patient II-1 and Patient I-1 all suffered from dysarthria until death, the details of which were unknown.

The present family demonstrated autosomal dominant inheretance of ALS and both sexes were affected. Six family members (patients I-1, II-1, II-4, II-5, III-2 and III-4) were suspected to have ALS, among whom three (II-5, III-2 and III4) had definite ALS according to the El-Escorial criteria. All six patients (2 men and 4 women) with familial ALS in this family showed dysarthria at the onset, so their clinical courses were indistinguishable from bulbar-onset ALS. There was no history of dementia and no atypical features in the kindred. Based on the information of the patients with good clinical records (patients II-4, II-5, III-2 and III-4), the mean age of symptom onset was 52.5 years (range 44-61 years) and the mean disease duration was 9.5 years (range

9-10 years) from symptom onset to death based on the outcome in patients II-4 and II-5.

After approval by the Ethics Committees of all participating institutions, sequencing of the coding regions of the TDP-43 gene in the patients (III-2 and III-4) was performed, which showed a heterozygous A-to-G transition at cDNA position 1009 (c.1009A>G) resulting in a methione-to-valine substitution at position 337 (M337V) in a highly conserved region of exon 6 (Fig. 1-2). None of the control 1,621 healthy subjects providing informed consent had this missense mutation.

Immunohistochemistry analysis of the brain of patient II-5 using both a phosphorylation-independent anti-TDP-43 antibody (10782-2-AP) and a phosphorylation-dependent anti-TDP-43 antibody (pS409/410) (8) showed neuronal cytoplasmic inclusions in the anterior horn of the spinal cord (Fig. 1-3A, B) and the hypoglossal nucleus (Fig. 1-3C), as well as glial cytoplasmic inclusions in the precentral gyrus (Fig. 1-3D, E).

Discussion

In the present study, we detected the M337V substitution in TDP-43 in a Japanese family with ALS, including one case confirmed at autopsy (patient II-5). We consider that this M337V substitution was associated with the disease, since M337V was present in two affected individuals from one generation and never in the control subjects, in addition to the fact that M337V substitution of TDP-43 has already been reported to segregate with ALS within two probably unrelated kindreds (2, 6). In a UK autosomal dominant ALS family carrying M337V substitution of TDP-43 reported by Sreedharan et al (2), three had limb-onset ALS and two had bulbar-onset ALS. The mean age of symptom onset was 47 years (range 44 to 52). Mean disease duration was 5.5 years (range 4 to 7) from symptom onset to death. The M337V mutation carrier in a US family with a strong family history of ALS reported by Rutherford et al (6) showed upper limb-onset ALS at 38 years of age, 6 years younger than the earliest onset age reported in the British M337V family (2). In the present paper, we show the first Japanese family with ALS carrying M337V substition of TDP-43, in which virtually all patients showed dysarthria at the onset, suggesting that their clinical courses were indistinguishable from bulbar-onset ALS. Among these UK, US and Japanese families carrying TDP-43 M337V mutation, the common features include no signs of dementia or other atypical features of ALS and past middle age onset of the disease. However, the signs at onset were different among these three families, and mean disease duration in the present Japanese family was longer than that in the UK family, indicating the phenotype of this mutation is quite variable. The identification of M337V in three genealogically unrelated ALS families further implies the pathogenicity of TDP-43 M337V mutation.

Regarding the pathogenecity of TDP-43 M337V mutation, Sreedharan et al (2) reported that mutant forms of TDP-43 (including M337V) fragmented *in vitro* more easily than wild-type TDP-43 and, *in vivo*, caused neuronal apoptosis and developmental delay in chick embryos, suggesting a pathophysiological link between TDP-43 and ALS. In addition, Rutherford et al (6) showed that biochemical analysis of TDP-43 in lymphoblastoid cell lines of carriers with TDP-43 mutations including M337V revealed a substantial increase in fragments possibly cleaved by caspase, including the ~25 kDa fragment, compared to control cell lines, supporting TDA-43 as a cause of ALS. Our immunohistochemical study showed TDP-43 positive cytoplasmic inclusions in the anterior horn cells of the spinal cord and in the hypoglossal nucleus, as well as glial cytoplasmic inclusions in the precentral gyrus, suggesting that a neuroglial proteinopathy was related to TDP-43. Further investigations including biochemical analysis using patients' fibroblasts or lymphoblastoid cells will be necessary to elucidate the mechanism by which TDP-43 contributes to ALS and to develop new drugs that block the pathological process related to TDP-43.

Acknowledgement

The authors thank Dr. Shuzo Shintani, Department of Neurology, Toride Kyodo Hospital and Dr. Kazuo Yoshizawa, Department of Neurology, National Hospital Organization Mito Medical Center for their clinical information on some patients of this family. This work was supported in part by grants from Ministry of Health, Labor, and Welfare, Japan and Ministry of Education, Culture, Science and Technology, Japan.

References

1. Gitcho MA, Baloh RH, Chakraverty S, et al. TDP-43 A315T mutation in familial motor neuron disease. Ann Neurol **63**: 535-538, 2008.
2. Sreedharan J, Blair IP, Tripathi VB, et al. TDP-43 mutations in familial and sporadic amyotrophic lateral sclerosis. Science **319**: 1668-1672, 2008.
3. Yokoseki A, Shiga A, Tan CF, et al. TDP-43 mutation in familial amyotrophic lateral sclerosis. Ann Neurol **63**: 538-542, 2008.
4. Kabashi E, Valdmanis PN, Dion P, et al. TARDBP mutations in individuals with sporadic and familial amyotrophic lateral sclerosis. Nat Genet **40**: 572-574, 2008.
5. Van Deerlin VM, Leverenz JB, Bekris LM, et al. TARDBP mutations in amyotrophic lateral sclerosis with TDP-43 neuropathology: a genetic and histopathological analysis. Lancet Neurol **7**: 409-416, 2008.
6. Rutherford NJ, Zhang YJ, Baker M, et al. Novel mutations in TARDBP (TDP-43) in patients with familial amyotrophic lateral sclerosis. PLoS Genetics **4**: e1000193, 2008.
7. Tsuchiya K, Shintani S, Nakabayashi H, et al. Familial amyotrophic lateral sclerosis with onset in bulbar sign, benign clinical course, and Bunina bodies: a clinical, genetic, and pathological study of a Japanese family. Acta Neuropathol **100**: 603-

607, 2000.
8. Hasegawa M, Arai T, Nonaka T, et al. Phosphorylated TDP-43 in frontotemporal lobar degeneration and amyotrophic lateral sclerosis. Ann Neurol **64**: 60-70, 2008.

doi:10.1016/j.jmb.2009.10.068 J. Mol. Biol. (2010) 395, 445–456

JMB

Available online at www.sciencedirect.com

ScienceDirect

ELSEVIER

Characterization of Inhibitor-Bound α-Synuclein Dimer: Role of α-Synuclein N-Terminal Region in Dimerization and Inhibitor Binding

Yoshiki Yamaguchi[1,2*†], Masami Masuda[3,4†], Hiroaki Sasakawa[1,5], Takashi Nonaka[3], Shinya Hanashima[2], Shin-ichi Hisanaga[4], Koichi Kato[1,5,6] and Masato Hasegawa[3*]

[1]*Department of Structural Biology and Biomolecular Engineering, Graduate School of Pharmaceutical Sciences, Nagoya City University, 3-1 Tanabe-dori, Mizuho-ku, Nagoya 467-8603, Japan*

[2]*Structural Glycobiology Team, Systems Glycobiology Research Group, Chemical Biology Department, RIKEN, Advanced Science Institute, 2-1 Hirosawa Wako, Saitama 351-0198, Japan*

[3]*Department of Molecular Neurobiology, Tokyo Institute of Psychiatry, 2-1-8 Kamikitazawa, Setagaya-ku, Tokyo 156-8585, Japan*

[4]*Molecular Neuroscience Laboratory, Graduate School of Science, Tokyo Metropolitan University, 1-1 Minami-Osawa, Hachioji-shi, Tokyo 192-0397, Japan*

[5]*Institute for Molecular Science, National Institutes of Natural Sciences, 5-1 Higashiyama, Myodaiji, Okazaki, Aichi 444-8787, Japan*

α-Synuclein is a major component of filamentous inclusions that are histological hallmarks of Parkinson's disease and other α-synucleinopathies. Previous analyses have revealed that several polyphenols inhibit α-synuclein assembly with low micromolar IC_{50} values, and that SDS-stable, noncytotoxic soluble α-synuclein oligomers are formed in their presence. Structural elucidation of inhibitor-bound α-synuclein oligomers is obviously required for the better understanding of the inhibitory mechanism. In order to characterize inhibitor-bound α-synucleins in detail, we have prepared α-synuclein dimers in the presence of polyphenol inhibitors, exifone, gossypetin, and dopamine, and purified the products. Peptide mapping and mass spectrometric analysis revealed that exifone-treated α-synuclein monomer and dimer were oxidized at all four methionine residues of α-synuclein. Immunoblot analysis and redox-cycling staining of endoproteinase Asp-N-digested products showed that the N-terminal region (1–60) is involved in the dimerization and exifone binding of α-synuclein. Ultra-high-field NMR analysis of inhibitor-bound α-synuclein dimers showed that the signals derived from the N-terminal region of α-synuclein exhibited line broadening, confirming that the N-terminal region is involved in inhibitor-induced dimerization. The C-terminal portion still predominantly exhibited the random-coil character observed in monomeric α-synuclein. We propose that the N-terminal region of α-synuclein plays a key role in the formation of α-synuclein assemblies.

*Corresponding authors. Y. Yamaguchi is to be contacted at Structural Glycobiology Team, Systems Glycobiology Research Group, Chemical Biology Department, RIKEN, Advanced Science Institute, 2-1 Hirosawa Wako, Saitama 351-0198, Japan. E-mail addresses: yyoshiki@riken.jp; masato@prit.go.jp.

† Y.Y. and M.M. contributed equally to this work.

Abbreviations used: PD, Parkinson's disease; Exi-monomer, exifone-bound monomer; Exi-dimer, exifone-bound dimer; HSQC, heteronuclear single quantum coherence; NBT, nitroblue tetrazolium; MALDI-TOF, matrix-assisted laser desorption/ionization time-of-flight; MS, mass spectrometry.

0022-2836/$ - see front matter © 2009 Elsevier Ltd. All rights reserved.

[6]*Okazaki Institute for Integrative Bioscience, National Institutes of Natural Sciences, 5-1 Higashiyama, Myodaiji, Okazaki, Aichi 444-8787, Japan*

Received 3 April 2009; received in revised form 26 September 2009; accepted 27 October 2009
Available online
3 November 2009

Edited by S. Radford

Keywords: NMR; α-synuclein; dimer; dopamine; Parkinson's disease

Introduction

Parkinson's disease (PD) and other α-synucleinopathies are progressive neurodegenerative diseases characterized by the selective loss of dopaminergic neurons and deposition of filamentous Lewy bodies, of which α-synuclein is the major component. Formation of amyloid fibrils and/or intermediate oligomers of α-synuclein is a complex process, and small-molecular inhibitors have been used to investigate the pathways involved. Conway *et al.* reported that catechol-containing compounds, including dopamine, inhibited the formation of α-synuclein fibrils, causing the accumulation of α-synuclein protofibrils.[1] It was also reported that α-synuclein fibrillization was inhibited by dopamine analogues, and α-synuclein oligomers were stabilized by these compounds.[2] We have previously reported that several polyphenols inhibited α-synuclein assembly with IC_{50} values in the low micromolar range, and that noncytotoxic, SDS-stable α-synuclein oligomers were formed in the presence of inhibitory compounds.[3]

Analyses of the interactions between small-molecular inhibitory compounds and α-synuclein have been reported by many groups, but the mechanisms involved remain controversial. It was proposed that amyloid fibril formation is inhibited by polyphenol compounds *via* noncovalent aromatic interactions with the amyloidogenic core.[4] A recent report showed that chemical aggregates inhibited amyloid formation of the yeast and mouse prion proteins in a manner characteristic of colloidal inhibition, suggesting a nonspecific mechanism.[5] Mutagenesis and competition studies with specific synthetic peptides suggested α-synuclein residues 125–129 (YEMPS) as an important region for dopamine-induced inhibition of α-synuclein fibrillization, and the inhibition was proposed to be due to conformational alterations of α-synuclein induced by noncovalent interaction with oxidized dopamine.[6] Molecular dynamics simulations suggest that dopamine binds to the YEMPS region, and the bound dopamine is further stabilized by long-range electrostatic interactions with E83 in the NAC region.[7] A recent NMR analysis indicated that a polyphenol compound, epigallocatechin gallate, noncovalently binds to the C-terminal region of α-synuclein (D119, S129, E130, and D135).[8] NMR analysis showed that A53T mutant α-synuclein, which is linked to autosomal dominant forms of PD, has a greater propensity to aggregate in the presence of dopamine, compared to wild-type α-synuclein.[9] Meanwhile, NMR characterization of the interaction between α-synuclein and various small molecules indicated that residues 3–18 and 38–51 act as noncovalent binding sites for inhibitory compounds.[10]

Covalent attachment of inhibitors to α-synuclein, on the other hand, has been proposed by several groups. Conway *et al.* suggested that 5–10% of dopamine was covalently incorporated into α-synuclein by radical coupling (dopamine-derived orthoquinone to Tyr) and/or nucleophilic attack (e.g., Lys forming a Schiff base with the orthoquinene).[1] Mass spectrometry (MS) and NMR characterization suggested that the oxidation product (quinones) of a dopamine analogue was covalently linked to the amino groups of the α-synuclein chain, thereby generating α-synuclein–quinone adducts.[2] Thus, the binding mode and binding site(s) of small-molecular inhibitors remain controversial.

The conformation of inhibitor-induced α-synuclein oligomers is also a matter of debate. Norris *et al.* reported that spherical oligomers of dopamine-modified α-synuclein take a predominantly random-coil structure with some β-pleated sheets on the basis of CD and Fourier-transform infrared spectroscopy studies.[6] Another group demonstrated that in the presence of small inhibitory molecules, α-synuclein is still dominated by random-coil character.[10] Ehrnhoefer *et al.* proposed that epigallocatechin prevented the conversion of monomeric α-synuclein into toxic on-pathway aggregation intermediates and resulted in the formation of unstructured, nontoxic α-synuclein oligomers that they considered to be off-pathway.[8] On the other hand, it has recently been reported that a flavonoid, baicalein, stabilized β-sheet-enriched oligomers based on CD and Fourier-transform infrared spectroscopy analysis.[11] The baicalein-stabilized oligomers were characterized as quite compact globular species based on small-angle X-ray scattering data and atomic force microscopy.

Masuda *et al.* isolated α-synuclein dimers formed in the presence of inhibitory compounds,[3] and the isolated soluble dimers were recently characterized using a panel of epitope-specific α-synuclein antibodies.[12] The reactivities of the antibodies indicated that the conformations of polyphenol-bound α-synuclein dimers differ from those of unbound monomers, but resemble those of amyloid fibrils, suggesting that inhibitor-bound molecular species are on-pathway intermediates.

This situation prompted us to carry out a comprehensive analysis of inhibitor-treated α-synucleins by means of NMR spectroscopy in conjunction with other biochemical methods, such as peptide mapping, immunoblotting, and redox-cycling staining. We have previously analyzed the antibody binding and site-specific phosphorylation of α-synuclein using ultra-high-field NMR spectroscopy.[13] For the structural characterization, we prepared and purified a ^{15}N-labeled α-synuclein dimer in the presence of polyphenol inhibitors on a milligram scale and analyzed it by ultra-high-field NMR spectroscopy recorded at a proton observation frequency of 920 MHz.

Results and Discussion

Isolation and characterization of inhibitor-bound α-synuclein dimer and monomer

SDS-stable, noncytotoxic α-synuclein oligomers were detected in the soluble fraction in the presence of inhibitory compounds such as polyphenols.[3] For detailed characterization of inhibitor-induced α-synuclein oligomers, we attempted to prepare exifone-, gossypetin-, and dopamine-induced α-synuclein dimer and monomer (for inhibitor structures, see Fig. 1) and to separate them by gel-filtration chromatography as described.[12] Fig. 2a shows the HPLC patterns of control and exifone-treated α-synucleins. The HPLC fractions of exifone-treated α-synuclein were analyzed by SDS-PAGE and Western blotting (Fig. 2b). The data indicate that the exifone-treated α-synuclein dimer (Exi-dimer) was successfully purified by gel-filtration chromatography. The homogeneity of inhibitor-induced monomer and dimer was also checked by diffusion NMR experiments (data not shown). α-Synuclein monomer and dimer treated with exifone, as well as control monomer (without inhibitor), were subjected to matrix-assisted laser desorption/ionization time-of-flight (MALDI-TOF) MS measurements (Fig. 2c). α-Synuclein monomer (control) showed a major signal at 14,460 Da, which matched the predicted mass (14,460 Da). On the other hand, exifone-treated monomer (Exi-monomer) gave a major signal at 14,524 Da, which corresponded to that of α-synuclein plus 64 Da. Exifone-bound α-synuclein (molecular mass of exifone, 278.2 Da) was not detected, presumably because exifone binding was noncovalent. The MS spectrum of Exi-dimer showed a broad peak at around 30 kDa and 15 kDa, and we could not obtain an accurate molecular mass. The peak at 15 kDa might be the doubly charged ion of the Exi-dimer and/or the monomer released from the Exi-dimer in the ionization process. To estimate the ratio of exifone bound to α-synuclein dimer and monomer, absorption of exifone at 385 nm was measured for Exi-dimer and Exi-monomer. The results indicate that Exi-dimer contains around 3

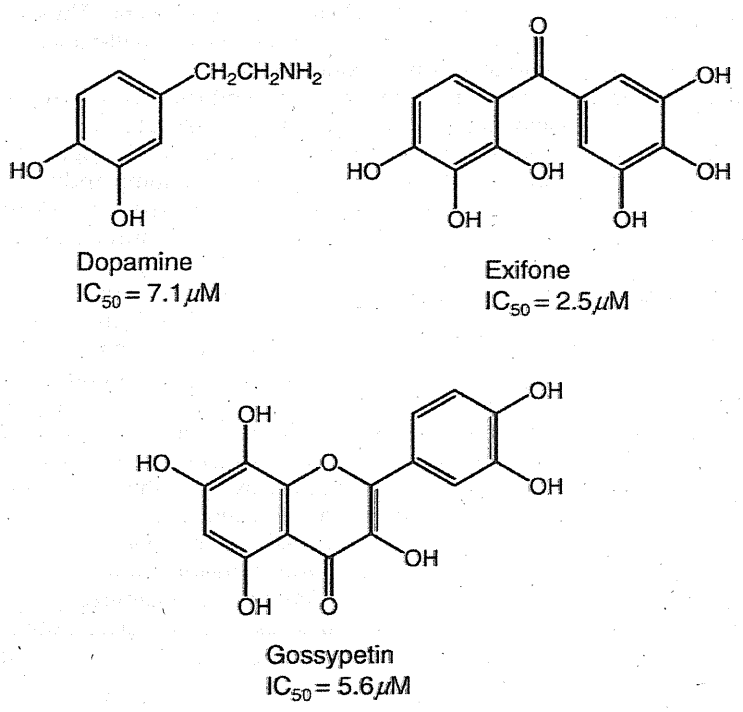

Fig. 1. Chemical structures of dopamine, exifone, and gossypetin with their IC_{50} values for inhibition of α-synuclein filament assembly.[3]

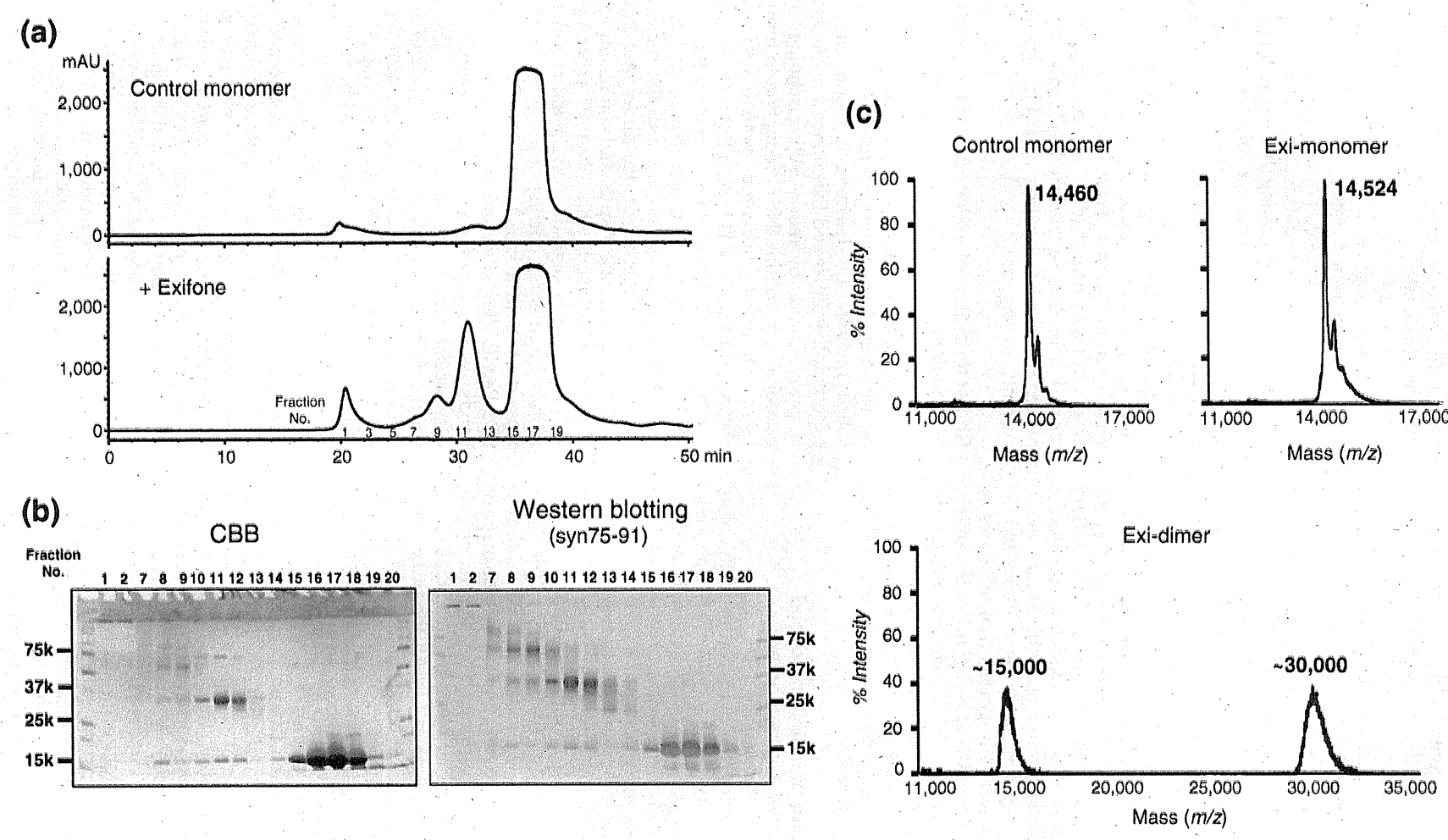

Fig. 2. Isolation and characterization of exifone-bound α-synucleins. (a) Separation of exifone-treated α-synuclein monomer and dimer by gel-filtration chromatography (detection: absorbance at 214 nm). (b) SDS-PAGE of fractions separated by gel-filtration chromatography (Coomassie brilliant blue staining and Western blotting). Pooled fractions 11–12 and 16–18 were used as Exi-dimer and Exi-monomer, respectively. (c) Partial MALDI-TOF MS spectra of α-synuclein monomer (control), Exi-monomer, and Exi-dimer.

molecules of exifone per α-synuclein monomer, while Exi-monomer contains one exifone molecule per α-synuclein chain (Supplementary Fig. S1).

For the identification of the modification (corresponding to a molecular mass of 64 Da) found in the Exi-monomer, α-synuclein was incubated with various concentrations of exifone (0, 0.2, 0.5, 1, and 2 mM) and the resulting samples were analyzed by MS (Supplementary Fig. S2). The molecular mass of α-synuclein increased in an exifone concentration-dependent manner and reached 14,528 Da (Supplementary Fig. S2a and b). A similar increase in molecular mass was reported in the presence of H_2O_2, which oxidized methionine residues to methionine sulfoxide.[14] Methionine oxidation is known to increase mass by 16 Da. α-Synuclein has four methionine residues, Met1, Met5, Met116, and Met127, and thus the oxidation of all the methionine residues would result in an increase in mass of 64 Da (Supplementary Fig. S3c). Indeed, α-synuclein incubated with various concentrations of H_2O_2 showed a concentration-dependent increase in molecular mass of up to 14,533 Da (Supplementary Fig. S3a and b), similar to that seen in the case of exifone. These results strongly suggest that all the methionine residues of Exi-monomer were oxidized to methionine sulfoxide.

Peptide mapping of inhibitor-induced α-synuclein dimer and monomer

In order to confirm the oxidation of methionine, control α-synuclein, Exi-monomer, Exi-dimer, and H_2O_2-treated α-synuclein monomer were digested with trypsin, and the resulting peptide mixtures were analyzed by reverse-phase HPLC (Fig. 3a). The elution patterns of peptides derived from Exi-monomer and Exi-dimer exhibited different profiles compared with that of control α-synuclein. Peaks 5 and 10 in the map of control α-synuclein were absent in the maps of Exi-monomer and Exi-dimer. Instead, peaks 11–18 newly appeared in the maps of Exi-monomer and Exi-dimer. The patterns of Exi-monomer and Exi-dimer were similar to those of α-synuclein oxidized with H_2O_2. All the peaks were analyzed by MS and the results are summarized in Fig. 3b. Peaks 5 and 10 were identified as Met1–Lys6 (containing two methionines, Met1 and Met5) and Asn103–Ala140 (containing Met116 and Met127), respectively. In the case of Exi-monomer or Exi-dimer, peaks 11, 15, and 19 were identified as Met1–Lys6 including two oxidized methionines. Peaks 12, 16, and 20 were identified as Asn103–Ala140 including oxidized Met116 and Met127. Peaks 13, 14, 16, and 17 were derived from Asn103–Ala140 oxidized at either Met116 or Met127. Similar results were obtained for dopamine-bound dimer and monomer (data not shown). These results clearly indicate that the inhibitors exifone and dopamine have the ability to oxidize methionine residues on α-synuclein. It is established that α-synuclein assembly was inhibited by exifone at low micromolar range (IC_{50}=2.5 μM),[3] and methionine sulfoxide could not be detected at a low concentration of exifone (data not shown). These findings suggest that the stabilization of intermediate oligomers by small molecules is responsible for the inhibition of filament formation, and oxidation of methionine does not seem to play a major role in inhibition.

No covalent inhibitor–peptide adducts or cross-linked peptides were detected in the peptide mapping experiments, indicating that the inhibitors bind noncovalently to α-synuclein and that α-synuclein dimer is formed in a noncovalent fashion. These observations are consistent with the results of MALDI MS analysis of Exi-monomer, which showed no inhibitor adducts (Fig. 2c). Our extensive liquid chromatography–electrospray ionization MS analysis also did not show the covalent inhibitor adducts or α-synuclein dimer (data not shown). Further, more detailed biochemical studies to investigate the modes of inhibitor binding and dimerization are currently in progress.

Characterization of exifone-binding regions in α-synuclein

Exifone is an antioxidant and thus can be detected by redox-cycling staining, which is a well-established method for detecting quinoproteins.[15] As expected, Exi-dimer and Exi-monomer were stained as purple bands by redox-cycling staining due to nitroblue tetrazolium (NBT) reduction to formazan (Fig. 4a), while untreated control α-synuclein showed no staining. This result shows that redox-cycling staining is useful for examining the exifone-binding regions in α-synuclein. In order to determine the binding region of exifone and the regions involved in the dimerization, Exi-dimer was digested with endoproteinase Asp-N and the resulting peptides were detected with silver or redox-cycling staining. Asp-N digestion of Exi-dimer gave two major fragments, corresponding to molecular masses of 20 kDa (no. 1) and 16 kDa (no. 2), on SDS-PAGE after silver staining (Fig. 4b). These two bands were positive for redox-cycling staining. Since α-synuclein monomer migrates at 15 kDa, these fragments represent dimeric peptides stabilized by exifone. α-Synuclein has six aspartic acid residues (Asp2, Asp98, Asp115, Asp119, Asp121, and Asp135). Immunoblot analysis with a panel of site-specific anti-α-synuclein antibodies (Fig. 5) suggested that the 20-kDa fragment contains the dimerized N-terminal fragment Met1–Met97 of α-synuclein (cleaved at the N-terminus of Asp98). The 16-kDa fragment was also labeled with antibodies to the N-terminal and central portions of α-synuclein (residues 1–50). It has been reported that Asp-N cleaves peptide bonds N-terminal to glutamate as well as aspartate residues.[16,17] Glu57 and/or Glu61 are found in the middle of α-synuclein and are candidate Asp-N cleavage sites to produce the 16-kDa fragment. The reactivity of anti-α-synuclein antibodies and the relaxed specificity of Asp-N indicate that the 16-kDa fragment corresponds to a dimer composed of Met1–Ala56/Lys60. These results suggest that the N-